

Model selection in electromagnetic production of kaons

Dalibor Skoupil^{1,*}, *Petr Bydžovský*¹, *Aleš Cieplý*¹, *Dimitrios Petrellis*¹, and *Denisa Trnková*^{1,2}

¹Nuclear Physics Institute, Czech Academy of Sciences, Řež, Czech Republic

²Faculty of Nuclear Sciences and Physical Engineering, Czech Technical University, Prague, Czech Republic

Abstract. New isobar models for the photoproduction of kaons off the proton target were constructed utilizing a consistent formalism for exchanges of high-spin resonances and energy-dependent widths of nucleon resonances. For adjusting the free parameters of the model to experimental data we employ regularization techniques, which prevent us from overfitting the data. We analysed the plentiful data on the $K^+\Lambda$ channel as well as the recent data on $K^+\Sigma^-$ channel and compare the results with data.

1 Introduction

The photoproduction and electroproduction of hyperons from nucleons are promising reactions for the study of the baryon resonance spectrum. One can obtain information about the so-called "missing resonances" that are predicted by quark models but have not been observed in the π or η meson production experiments. These resonant states may not have been detected because of their strong decay to the $K\Lambda$ and $K\Sigma$ channels. A description of the elementary processes can also be easily implemented to the study of production of hypernuclei whereby one can gain more understanding of hyperon-nucleon and hyperon-hyperon interactions.

A variety of theoretical studies of the hyperon production have been performed in the last couple of decades, with a particular emphasis on the $K^+\Lambda$ photoproduction. This process was initially studied in the 1960s, while more experimental data became available in the 1980s and 1990s, which led to increased interest of theoreticians. Besides many others, the group at Ghent University examined the role of background contributions to the $K^+\Lambda$ photoproduction, as well as the effects of hyperon resonances contributing to the process [1]. The data on differential cross sections and polarization observables measured by the CLAS Collaboration [2] were utilized by the Ghent group to create a model describing the $p(\gamma, K^+)\Lambda$ around the threshold and at high energies [3, 4]. Currently, there are only a few experimental data on differential cross sections measured with the use of neutron targets [5–8]. Only two measurements of the beam asymmetry Σ in the $K^+\Sigma^-$ channel are at present available, one measured by the LEPS collaboration [5] and the other, more recent, by the CLAS collaboration [9], which covers a broad spectrum of kinematics.

The processes are described by using isobar models based on effective Lagrangians, and the number of model parameters is proportional to the amount of resonances considered. The

*e-mail: skoupil@ujf.cas.cz

well-known feature of the isobar models is the unphysically large values of hyperon couplings, such as in the case of Saclay-Lyon model [10], or our models BS1 and BS2 [11] created in 2016 by utilizing currently available data. Newly, we have used a fitting technique penalizing unphysically large values of free model parameters. In statistics, these regularization techniques are widely employed to create models describing the data more properly and to prevent overfitting. By using the Ridge regularization, we are able to deal with the problem of too large values of hyperon coupling constants. The Ridge regularization also lets us work with a chosen set of resonances while shrinking the free parameters.

2 Methodology

2.1 Isobar model

In this work, we make use of the isobar model in which we construct the amplitude from effective meson-baryon Lagrangians. The non-resonant part of the amplitude is made up of exchanges of the ground-state hadrons and exchanges of kaon and hyperon resonances in the t and u channel, respectively. The resonant part is then modelled by the exchanges of nucleon resonances in the s channel. In our approach, we neglect any contributions beyond the tree-level order (*e.g.* rescattering and final-state interactions). As none of the exchanged particles is point like, we introduce a hadronic form factor in the strong vertex which mimics the internal structure [11].

Among the most important ingredients of our model belongs a so-called consistent formalism for the exchange of high-spin resonances. In this formalism, non-physical degrees of freedom, which are connected to lower-spin content of high-spin fermion fields, vanish in the amplitude. In order to restore unitarity, which is broken by working at the tree level only, we use the energy-dependent decay widths of nucleon resonances [12].

2.2 Adjusting model parameters to data

Fitting a theoretical model to experimental data involves finding the values of the model's parameters that minimize a certain error function. Even though the use of complex models, which have a large number of parameters, can result in very low errors, more often than not it makes the minimization procedure unstable, yielding many similar minima corresponding to wildly varying values of the parameters. Thus, reducing the magnitude and/or the number of the model's parameters becomes particularly important.

The standard tool used in such cases is called regularization which involves inclusion of a penalty term in the error function that prevents the parameters from taking extreme values. The penalty term contains an L_q norm of the parameter vector and thus, in effect, converts the problem of error minimization to the one of constrained minimization. When $q = 1$ and 2 , we speak of L_1 and L_2 norms, respectively, with L_1 limiting both the number of parameters as well as their magnitudes and L_2 limiting only their magnitudes. The penalization with the L_2 norm gives us Ridge regression with a smooth objective function but with poor parameter pruning ability. Using the L_1 norm, we obtain Least Absolute Shrinkage Selection Operator (LASSO) estimation technique which has good pruning behaviour but the non-smooth objective function causes optimization difficulties.

In our work, we upgraded the fitting procedure for adjusting free parameters and opted for the LASSO technique to avoid the problem of overfitting the data, which leads to minimizing the amount of introduced parameters. We employed this technique, together with information criteria to select the most appropriate model, for the analysis of $K^+\Sigma^-$ channel [13] and $K^+\Lambda$ channel (although these results are still preliminary). We also made use of the Ridge

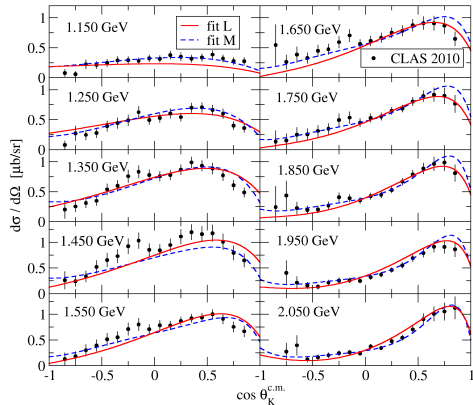


Figure 1: The differential cross section of the $\gamma n \rightarrow K^+\Sigma^-$ process as a function of cosine of the kaon center-of-mass angle $\theta_K^{c.m.}$ for several photon lab energies E_γ^{lab} . The data are from Ref. [8]. The fits L and M are represented by solid and dashed lines, respectively.

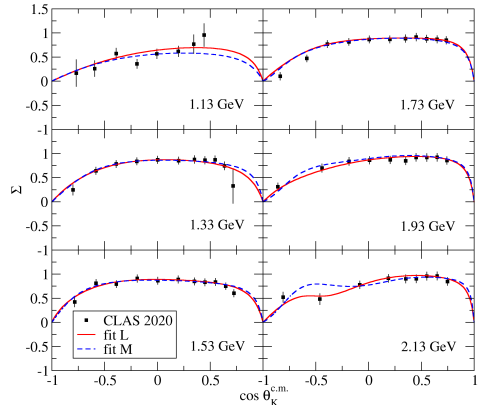


Figure 2: The photon-beam asymmetry of the $\gamma n \rightarrow K^+\Sigma^-$ process as a function of cosine of the kaon center-of-mass angle $\theta_K^{c.m.}$ for several photon lab energies E_γ^{lab} . The data are from Ref. [9]. The fits L and M are represented by solid and dashed lines, respectively.

regression in order to keep resonances' couplings within their natural limits in the reanalysis of data in the $K^+\Lambda$ channel [14].

3 Results and discussion

Firstly, we focused on the $K^+\Sigma^-$ channel and adjusted the free parameters of the model to available data (we fitted around 20 parameters to 674 data points). We concluded the fitting process with two models. One of them was achieved by minimizing the χ^2 without regularization (we dubbed this model "fit M") and the other model resulted from minimizing the penalized χ^2 as described above (this model is called "fit L"). There are 14 resonances and 25 parameters in fit M, whereas in the fit L there are only 9 resonances and 17 free parameters. Even though the use of LASSO produces a slight increase in the χ^2 value, it clearly leads to a more economical fit, which is still in a very good agreement with the experiment. Calculations of differential cross sections and photon-beam asymmetry by both fit M and fit L are shown and compared to data in Figs. 1 and 2, respectively. These results show that the role of hyperon resonances for reliable data description is rather small since there are no hyperon resonances included in the new fits.

The next step was to focus again at the $K^+\Lambda$ channel, this time with the enhanced χ^2 minimization. Using the Ridge regression, we were able to reduce hyperon couplings which in previous studies reached unreasonably large values (more details given in Ref. [14]). This study therefore can shed a new light on the role played by hyperon resonances in the $K^+\Lambda$ photoproduction. Model calculations are compared with data in Fig. 3.

Very recently, we employed also the LASSO technique for the study of the $K^+\Lambda$ channel. Similarly to the analysis using the Ridge regression, we could find an economical fit with no hyperon resonances which is in a good agreement with data (results are shown in Fig. 4).

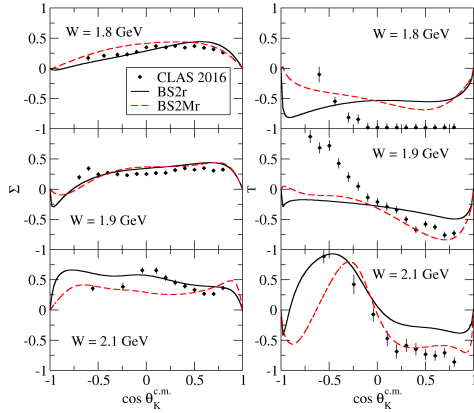


Figure 3: Photon-beam asymmetry (left) and target asymmetry (right) of the $\gamma p \rightarrow K^+ \Lambda$ process in dependence on the cosine of the kaon center-of-mass angle $\theta_K^{c.m.}$ for several values of invariant energy W . The data stem from Ref. [15], refits of the BS2 model are denoted by solid and dotted lines.

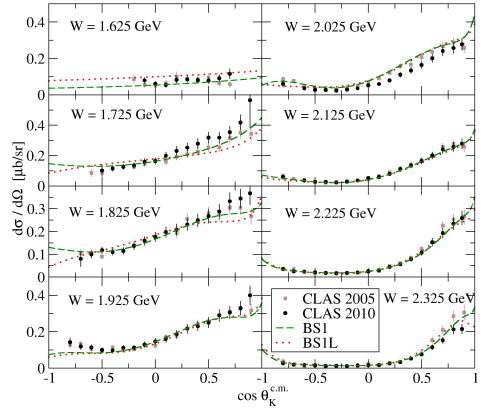


Figure 4: The differential cross section of the $\gamma p \rightarrow K^+ \Lambda$ process in dependence on the cosine of the kaon center-of-mass angle $\theta_K^{c.m.}$ for several values of W . The data stem from Refs. [2, 16]. The BS1 model is denoted by dashed line and the its refit (BS1 L) by dotted line.

4 Conclusion

We described the process of photoproduction of kaons on protons within the framework of an isobar model. In order to avoid overfitting and to select the appropriate models, we turned to regularization techniques. We show results of our studies of the $K^+ \Lambda$ and $K^+ \Sigma^-$ channels and compare behaviour of our models with experimental data.

References

- [1] S. Janssen, J. Ryckebusch, D. Debruyne, and T. Van Cauteren, Phys. Rev. C **65**, 015201 (2001), S. Janssen, *et al.*, Eur. Phys. J. A **11**, 105 (2001).
- [2] R. Bradford *et al.*, Phys. Rev. C **73**, 035202 (2006).
- [3] T. Corthals, J. Ryckebusch, and T. Van Cauteren, Phys. Rev. C **73**, 045207 (2006).
- [4] L. De Cruz, J. Ryckebusch, T. Vrancx, P. Vancraeyveld, Phys. Rev. C **86**, 015212 (2012).
- [5] H. Kohri *et al.* (LEPS Collaboration), Phys. Rev. Lett. **97**, 082003 (2006).
- [6] K. Tsukada *et al.*, Phys. Rev. C **78**, 014001 (2008).
- [7] K. Kohl *et al.* (BGOOD Collaboration), arXiv:2108.13319v2 [nucl-ex].
- [8] S. A. Pereira *et al.* (CLAS Collaboration), Phys. Lett. B **688**, 289 (2010).
- [9] N. Zachariou *et al.* (CLAS Collaboration), Phys. Lett. B **827**, 136985 (2022).
- [10] J. C. David, C. Fayard, G.-H. Lamot, and B. Saghai, Phys. Rev. C **53**, 2613 (1996).
- [11] D. Skoupil, P. Bydžovský, Phys. Rev. C **93**, 025204, (2016).
- [12] D. Skoupil, P. Bydžovský, Phys. Rev. C **97**, 025202, (2018).
- [13] P. Bydžovský *et al.*, Phys. Rev. C **104**, 065202 (2021).
- [14] D. Petrellis, D. Skoupil, Phys. Rev. C **107**, 045206 (2023).
- [15] C. A. Paterson *et al.* (CLAS Collaboration), Phys. Rev. C **93**, 065201 (2016).
- [16] M. E. McCracken *et al.* (CLAS Collaboration), Phys. Rev. C **81**, 025201 (2010).